Characterising Silicone Rubber: Indentation and Dynamic Modelling

Kamogelo D. Malatsi[a], Gerhard Venter[b]

Received 11 March 2025, in revised form 15 September 2025 and accepted 17 November 2025

Abstract: ***Rubber's unique elastic and viscous properties make it essential in engineering applications, particularly in industries such as automotive, construction, and mining. For example, in mining, vibrating screens often experience excessive vibrations during start-up and shutdown, potentially damaging machinery and reducing lifespan. Effective vibration isolators are crucial to mitigate this risk. This study presents a hyper-viscoelastic model for silicone rubber, combining the Mooney-Rivlin model for hyperelastic behaviour and the Generalised Maxwell model for time-dependent viscoelastic properties. Hyperelastic parameters were derived through inverse Finite Element (FE) modelling using indentation experiments with Digital Image Correlation (DIC) data. In contrast, viscoelastic parameters were obtained from stress relaxation tests via least-squares fitting. Validation through physical testing and FE simulations demonstrated the validity of the obtained material model and the significant influence of the viscoelastic effects on the dynamic behaviour. The validation data also show a loss in accuracy from the material model at high frequencies, as one would expect from a quasi-static relaxation test.***

Additional keywords: Hyper-viscoelastic, Indentation test, Relaxation test

Nomenclature

FE	Finite element
DIC	Digital image correlation
FEMU	Finite element update method

[a] ORCID 0009-0002-1346-1175. Stellenbosch University. Department of Mechanical and Mechatronic Engineering, Stellenbosch University, Private Bag X1, Matieland, Stellenbosch, 7602, Western Cape, South Africa. E-mail: malatsikamogelo48@gmail.com

[b] ORCID 0000-0001-9513-9774. Stellenbosch University. Department of Mechanical and Mechatronic Engineering, Stellenbosch University, Private Bag X1, Matieland, Stellenbosch, 7602, Western Cape, South Africa. E-mail: gventer@sun.ac.za

1 Introduction

Rubber is a general term for macromolecular substances, either of natural origin (natural rubber) or synthetic origin (synthetic rubber). The primary chemical components of rubber are elastomers, which are long-chain-like molecules that can be stretched significantly and still return to their original shape. Silicone rubbers are a distinct class of elastomers derived from high-molecular-weight polyorganosiloxanes [1].

Hyperelasticity refers to materials that can undergo substantial elastic deformation and fully recover their original shape. These hyperelastic materials exhibit nonlinear elastic behaviour, meaning their stress response varies significantly with strain. Traditional linear stress-strain theories, such as Hooke's law, are insufficient for describing the behaviour of hyperelastic materials under stress, and more advanced models are required. Therefore, more suitable models known as hyperelastic constitutive models are used to describe this complex behaviour. Common hyperelastic models include the Neo-Hookean, Mooney-Rivlin, Ogden, Yeoh, and Arruda-Boyce models [2]. To account for the time-dependent behaviour of rubber, a viscoelastic rheological model is required. Some widely used viscoelastic models include the Maxwell, Kelvin, and Burger models, as well as the Generalised Maxwell model [3].

In a study by Li et al. [4], rectangular rubber specimens were utilised and uniaxial tension experiments were performed to determine the hyperelastic material properties for a two-term Mooney-Rivlin model. Dhakad et al. [5] investigated the hyperelastic properties of Hydrogenated Nitrile Butadiene Rubber (HNBR) with a 62 Duro Shore A hardness and Polychloroprene Rubber (PCR) with a 55 Duro Shore A hardness by conducting uniaxial and planar tests to characterise them with a three-parameter Mooney-Rivlin model. In contrast, Van Tonder et al. [6] developed a single, complex test to characterise rubber materials. This method involves examining the full-field displacement of the sample and applying a FE method update (FEMU) technique, enabling a complete material characterisation from a single test.

Building on these studies, Rey et al. [7] explored the behaviour of filled and unfilled silicone rubber, demonstrating that filled silicone rubber exhibits higher viscosity than unfilled silicone rubber. Given that the silicone rubber selected for this study is unfilled, a low viscoelastic response is expected.

In this paper, the authors present a hyper-viscoelastic model to characterise the properties of silicone rubber accurately. The study utilises the three-parameter Mooney-Rivlin model to describe the hyperelastic behaviour of silicone rubber, combined with experimental tests and FEMU to determine the

http://dx.doi.org/10.69694/2309-8988/2025/v41a4
http://www.saimeche.org.za (open access) © CC BY 4.0

material parameters. To capture rate-dependent behaviour, a four-parameter Generalised Maxwell viscoelastic model is applied, using the Prony series under stress-relaxation conditions. Silicone rubber was selected for its ease of use, but the work provides a methodology that can be applied to other types of rubber as well.

2 Constitutive models

2.1 Hyperelastic material model

Hyperelastic materials exhibit nonlinear elastic behaviour, meaning that their response to stress changes significantly with strain. Hyperelastic constitutive models capture this complex behaviour by describing the material's elastic properties through the strain energy density function W. The energy density can be described by three principle stretch ratios typically denoted as λ_1, λ_2 and λ_3. Stretch is defined as the ratio of the deformed length to the original length. The three stretch ratios are related to the principle strain invariants I_1, I_2 and I_3 as follows:

$$\begin{aligned} I_1 &= \lambda_1^2 + \lambda_2^2 + \lambda_3^2 \\ I_2 &= \lambda_1^2\lambda_2^2 + \lambda_2^2\lambda_3^2 + \lambda_3^2\lambda_1^2 \\ I_3 &= \lambda_1^2\lambda_2^2\lambda_3^2 = J^2 \end{aligned} \tag{1}$$

where J is the volumetric stretch ratio $\frac{V_F}{V_0}$.

The Mooney-Rivlin model is a hyperelastic material model often used to describe the nonlinear stress-strain behaviour of rubber-like materials, where the strain energy density function W governs the material behaviour. The strain energy density function for a three-term Mooney-Rivlin material is given as follows [2]:

$$W = C_{10}(I_1 - 3) + C_{01}(I_2 - 3) + C_{20}(I_1 - 3)^2 + D(J-1)^2 \tag{2}$$

where C_{10}, C_{01} and C_{20} are the Mooney-Rivlin parameters and I_1, I_2 and I_3 represent the strain invariants. The component $D(J-1)^2$ accounts for material compressibility, while the variable D represents the bulk modulus.

2.2 Viscoelastic material model

Hyperelastic material models can only describe a material's purely elastic properties, making them most suitable for static or quasi-static simulations. To model the time-dependent behaviour of rubber, generalised Maxwell mechanical models have been proposed. This approach consists of multiple Maxwell elements, collectively referred to as a Generalised Maxwell Model. From the solution for the stress relaxation and the relaxation modulus, the normalised shear relaxation modulus can be expressed using the Prony series. In its general form, the Prony series may include many terms and corresponding decay parameters, however, for this study, the two-term representation was adopted, given by:

$$g_R(t) = 1 - g_1(1 - e^{\frac{-t}{\tau_1}}) - g_2(1 - e^{\frac{-t}{\tau_2}}) \tag{3}$$

where g_1, g_2, τ_1 and τ_2 are the material parameters used to describe the viscoelastic nature of rubber [5]. The Prony series provides the solution to the Generalized Maxwell model.

3 Hyper-viscoelastic model

To better understand the mechanical behaviour of elastomeric materials, researchers typically combine hyperelastic and viscoelastic models in a parallel fashion as shown in Figure 1. Hajhashemkhani et al. [8] developed an inverse algorithm to identify material parameters of a hyper-viscoelastic model under unknown boundary conditions, using the Neo-Hookean model for hyperelasticity and a two-parameter Maxwell model with a Prony series for viscoelasticity under plane strain conditions. Li et al. [4] proposed a hyper-viscoelastic model for rubber by combining a hyperelastic element with a six-parameter Generalised Maxwell model, determining parameters through tensile creep experiments and uniaxial tensile tests. Dhakad et al. [5] investigated hyper-viscoelastic models for two elastomers, separating hyperelastic and viscoelastic components, and employed a four-parameter Generalised Maxwell model under stress relaxation tests, achieving strong correlation with experimental data. All hyperelastic models, except the Van der Waals model, demonstrated stability across all strain levels.

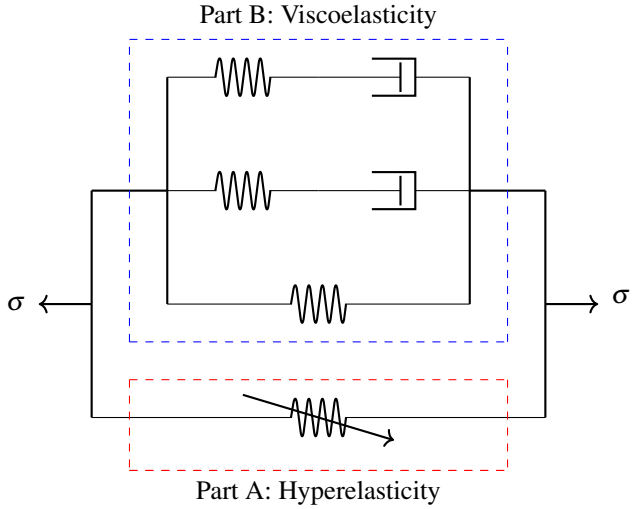

Figure 1 Hyper-viscoelastic model (Adapted from Dhakad et al. [5])

The total stress of the hyper-viscoelastic model is the sum of the stresses developed in parts A and B in Figure 1.

4 Material characterisation

Hyperelastic and viscoelastic properties can be characterised separately. These characterised material models are then combined into a single material model in the FE modelling software. In this study, Smooth-Sil 950 silicone rubber with a Shore 50 A hardness was used for characterisation. To ensure consistency across all test specimens, the silicone rubber was cast from a single batch. The samples were prepared by mixing two liquid components to form the silicone rubber. The mixture was degassed twice: once immediately after adequately mixing the two liquids and again after being poured into aluminium moulds, to eliminate any air bubbles. Aluminium moulds of various geometries were used to cast the samples for material characterisation. Silicone rubber was se-

http://dx.doi.org/10.69694/2309-8988/2025/v41a4
http://www.saimeche.org.za (open access) © CC BY 4.0

lected due to its ease of use, but it may not accurately represent the properties of the rubber used in vibrating screens. Therefore, the thesis aims to lay down a methodology that can be used for other types of rubber in future.

4.1 Hyperelastic characterisation

To determine the hyperelastic parameters of the silicone rubber, an indentation test with DIC was performed. The silicone rubber was cast into a 40 mm × 40 mm × 120 mm aluminium mould, as shown in Figure 2.

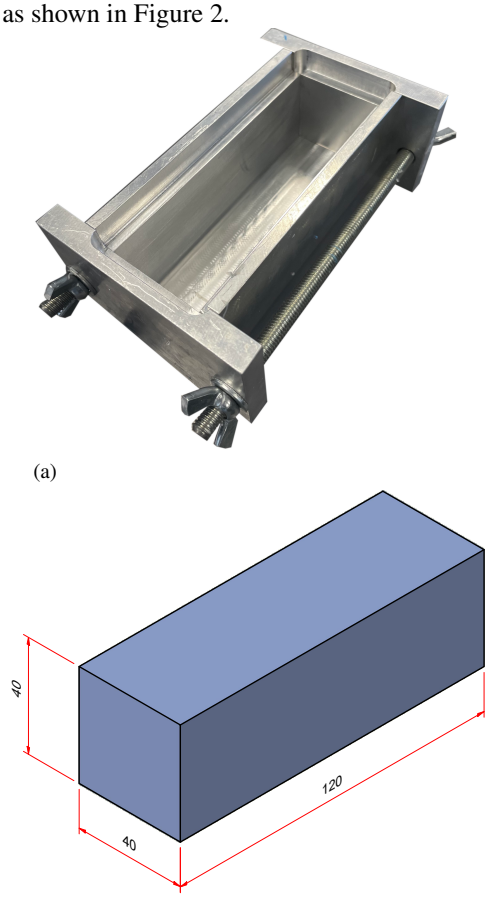

(a)

(b)

Figure 2 Aluminium mould (a) and sample geometry (b) for hyperelastic characterisation, with the dimensions in mm.

The test setup for the hyperelastic characterisation of the silicone rubber sample is illustrated in Figure 3. The setup included a tensile/compression test machine, an indenter, a compression plate, and a load cell to measure the indentation force. Additionally, a DIC system was used to capture the deformation of the rubber sample. DIC requires a distinct pattern on the sample surface that can be effectively correlated across photographs in a test. This is accomplished by applying a unique random pattern of paint speckles onto the sample surface. The speckle pattern was applied using black vinyl spray paint. The light blue silicone rubber provided sufficient contrast with the black speckles. Prior to commencing the tests, all surfaces in contact with the sample were lubricated using silicone lubricant to minimise friction.

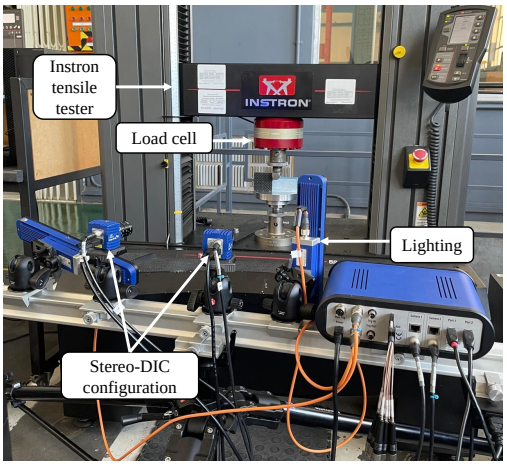

(a)

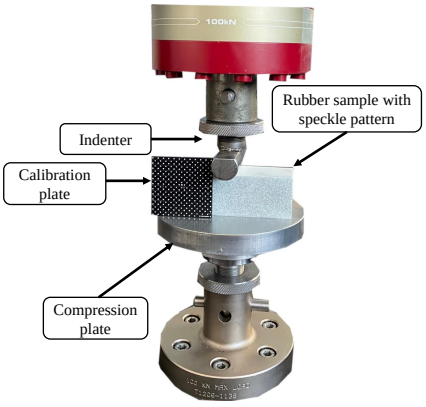

(b)

Figure 3 Hyperelastic material characterisation test setup. (a) Full experimental setup illustrating the DIC system and indentation test configuration. (b) Zoomed-in view highlighting the rubber sample under indentation.

The sample underwent indentation to a total displacement of 20 mm, at a consistent rate of 5 mm min^{-1}. This indentation depth was chosen because it covers the expected strain range in the application. The loading speed was selected to maintain quasi-static conditions throughout the test. To reduce the Mullins effect, the rubber sample was preconditioned at a strain level higher than the actual test [9]. The preconditioning graph is shown in Figure 4. A total of 7 preconditioning cycles were performed, and data collection was conducted only after the 7th cycle.

To accurately characterise the silicone rubber material, a numerical analysis as outlined by Van Tonder et al. [6] was required to establish the necessary material parameters. This involved selecting the three-parameter Mooney-Rivlin model as a suitable hyperelastic model to accurately reflect the material's behaviour, constructing an FE model to replicate the experimental indentation test and implementing a numerical approach to derive the material parameters. The same approach can be used for higher-order Mooney-Rivlin models, but the three-term model was sufficient to capture the data.

http://dx.doi.org/10.69694/2309-8988/2025/v41a4
http://www.saimeche.org.za (open access) © CC BY 4.0

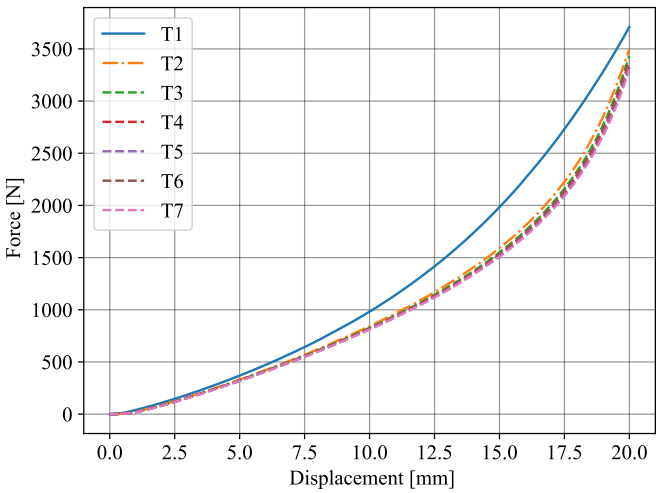

Figure 4 Rubber sample preconditioning and eventual indentation force curve convergence

4.2 Viscoelastic characterisation

To characterise the viscoelastic behaviour, a relaxation test was performed following the procedure given in BS ISO 6914:2021 [10]. The standard outlines a method for determining the ageing characteristics of vulcanised or thermoplastic rubber by measuring stress relaxation under tension. Dumbbell-shaped silicone rubber samples of Type 1A, as outlined in BS ISO 37:2017 [11], were cast in an aluminium mould to perform the relaxation tests. The aluminium mould and rubber sample geometry are illustrated in Figure 5.

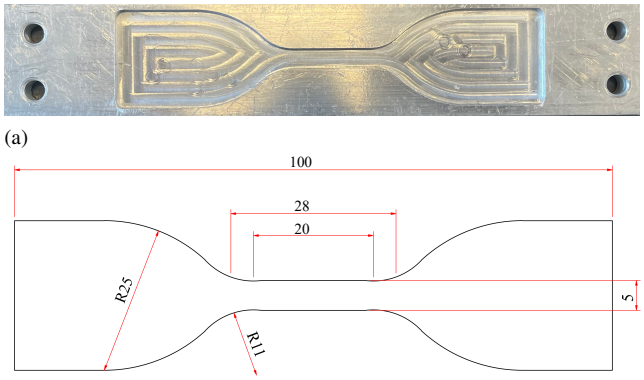

Figure 5 (a) Dumb-bell shaped aluminium mould. (b) Rubber sample geometry used for viscoelastic characterisation, with dimensions in mm.

The test setup for the viscoelastic material characterisation is illustrated in Figure 6. For the relaxation test, roller grips were used to prevent specimen slippage during testing. The grips are specifically used for silicone rubber and are supplied by the manufacturer. A long-travel extensometer was employed to accurately measure the specimen displacement to the required elongation for each test. A 1 kN load cell was selected to ensure accurate force measurement with minimal noise interference. The relaxation tests were conducted at room temperature, in accordance with the guidelines outlined in the standards [10].

Before conducting the relaxation tests, the dumbbell-shaped silicone rubber samples were preconditioned through several loading cycles. Preconditioning was conducted at a strain level above the test strain to ensure material stability prior to the test. The dumbbell-shaped specimens were elongated to a predefined displacement at a constant strain rate of 50 mm min^{-1}, and the crosshead movement was stopped once the target percentage elongation was reached. According to the testing standards [10], the test sample must be stretched to an elongation of 45 % to 55 %. To meet this requirement, a target of 50 % elongation was chosen. This range was monitored using an extensometer to maintain consistent elongation across all tests. The force data was measured at a sampling rate of 1 Hz.

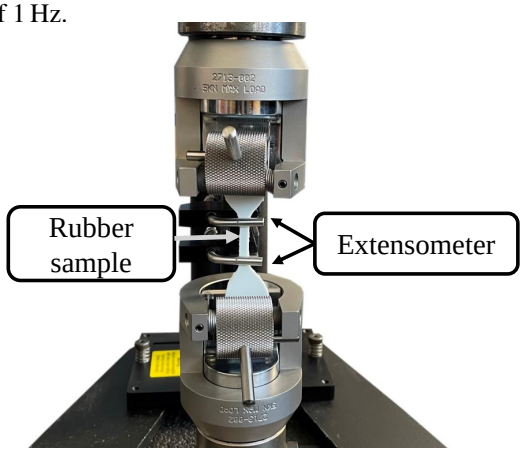

Figure 6 Relaxation test configuration showing the rubber sample with the long-travel extensometer attached

The four-parameter Generalised Maxwell model was chosen to characterise the viscoelastic properties of the silicone rubber material. Based on the literature, the four-parameter model was selected as a starting point that could be updated to a more parameterised model if needed, based on the experimental data [5]. Three dumbbell-shaped silicone rubber samples were used for the relaxation tests.

Once the experimental stress-relaxation data were collected, the Generalised Maxwell model was used to fit the data and derive the material parameters. The stress relaxation data was processed to improve its quality and reduce noise by applying a moving-average filter using a rolling window with a window size of 3. This choice of window size was made to balance the need for smoothing the data while preserving the underlying trends. The stress relaxation data were normalised, and least-squares fitting was performed to obtain the optimal model parameters for the Prony series, as given in Equation 3.

4.3 Material characterisation results

The aluminium material and the material parameters obtained from the hyperelastic and viscoelastic characterisation are summarised in Table 1. The Mooney-Rivlin parameters are obtained by FEMU and the viscoelastic parameters are obtained from relaxation tests and modelled using the four-term Generalised Maxwell model.

http://dx.doi.org/10.69694/2309-8988/2025/v41a4
http://www.saimeche.org.za (open access) © CC BY 4.0

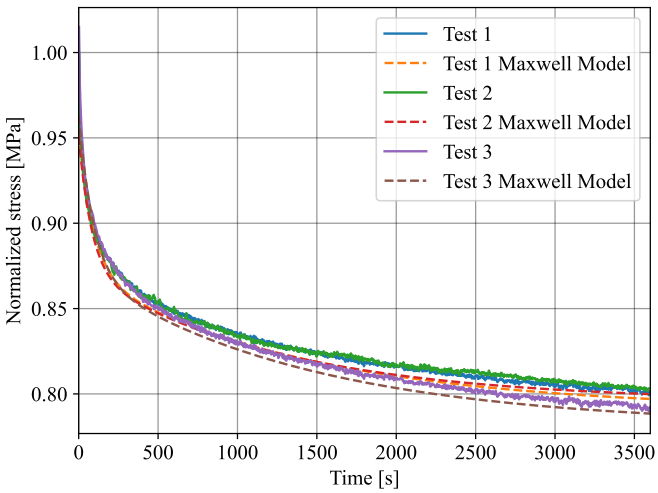

Figure 7 Normalised stress plot, comparing experimental data from three tests with the corresponding Generalised Maxwell model predictions for silicone rubber material over time

Table 1 Material properties

Aluminium density		2740 kg m^{-3}
Young's modulus		71.17 GPa
Poisson's ratio		0.33
Rubber density		1250 kg m^{-3}
Mooney-Rivlin	C_{10}	0.3757 MPa
	C_{01}	0.0139 MPa
	C_{20}	0.0867 MPa
Viscoelastic (Prony series)	g_1	0.1310
	τ_1	89.271
	g_2	0.0852
	τ_2	1365
Bulk modulus		3.8582 GPa

5 Experimental test validation

5.1 Physical experiment

To validate the obtained hyperelastic and viscoelastic material parameters, a physical experiment was conducted to determine the dynamic behaviour of the silicone rubber material. The physical experiment simulates a simple vibration isolator with a mass applied at the top. The physical test consisted of applying a base acceleration to a custom-designed, manufactured vibration isolator. The design includes two aluminium end caps, one at the top and one at the bottom of the silicone rubber specimen. The end caps were designed with an internal groove to prevent the aluminium from separating from the silicone rubber during testing. Additionally, aluminium pins were incorporated as a mechanical interlock. The physical test setup is illustrated in Figure 8.

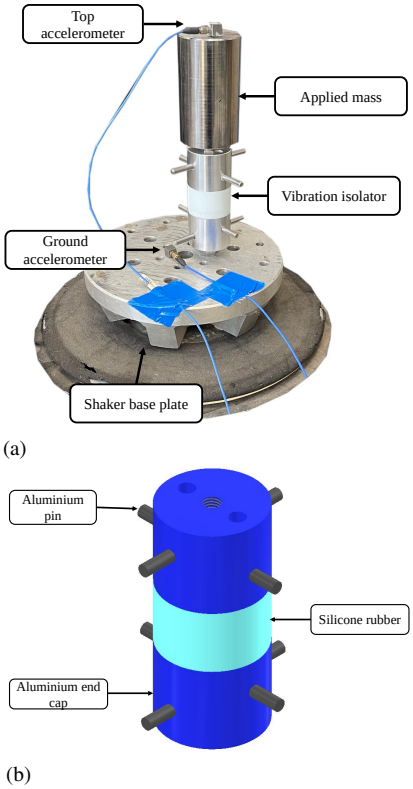

Figure 8 Vibration isolator test system. (a) Physical experimental setup. (b) FE representation of the vibration isolator

The physical experiment test setup included a Siemens DAQ (Data Acquisition) system and a PC with Simcenter Testxpress software. The DAQ acquired data from the Testxpress environment and output the generated signal to an LDS amplifier. The amplifier increased the signal to a level that could drive a shaker, causing it to vibrate. The shaker was set to perform a sine wave at 5 Hz for 20 s, after which the data was recorded. This process was repeated at increasing frequencies 10 Hz, 15 Hz, and continuing in this manner until 25 Hz. These frequencies were selected to ensure that the strain rates tested are aligned with those expected in the system's normal operating conditions. The experiment used two PCB 333B32 shear accelerometers, which were connected to a DAQ to measure vibration response. One accelerometer was placed on the shaker base plate to measure ground acceleration, and another was placed on top of the attached mass to measure the system's response. The accelerometers had sensitivities of 10.39 mV ms^{-2} and 9.96 mV ms^{-2}and were calibrated before the start of the test. The accelerometers, with a dynamic range of ±490 m s^{-2}, were sampled at 256 Hz with a bandwidth of 128 Hz. According to the Nyquist theorem, which states that the sampling frequency must be at least twice the highest frequency present in the signal to avoid aliasing, the chosen sampling rate of 256 Hz was sufficient.

5.2 Virtual experiment

The proposed hyper-viscoelastic material model was implemented in a nonlinear FE code to characterise the dynamic behaviour of the silicone rubber material using the obtained

http://dx.doi.org/10.69694/2309-8988/2025/v41a4
http://www.saimeche.org.za (open access) © CC BY 4.0

material parameters. A virtual experiment was performed in Hexagon Marc to simulate the physical experiment. The FE model was created to accurately replicate the physical experimental test.

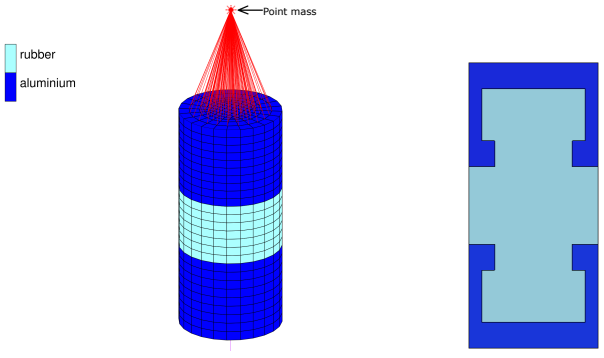

Figure 9 FE model of the vibration isolator. In image (a), Rigid elements (RBE3's) are seen applied at the top surface of the isolator to distribute forces evenly, with a point mass attached to simulate the applied mass. Image (b) shows the half-section view of the FE model

The aluminium end caps were designed with threaded holes. The top threaded hole facilitated attachment of a 2.14 kg mass via a bolt, while the bottom threaded hole was used to mount the vibration isolator to the shaker. The aluminium was modelled in Hexagon Marc using an elastic-plastic isotropic material property and its Young's modulus, Poisson's ratio and density were obtained from literature [12], also summarised in Table 1. The silicone rubber material was modelled using the three-parameter Mooney-Rivlin model as in Equation 2. The material is almost incompressible, and Hexagon Marc, by default, estimates the bulk modulus to be 5000 times the initial shear modulus. The viscoelastic material properties were given by a two-term Prony series. The density of the silicone rubber was determined by weighing the sample block and dividing the weight by its volume, as shown in Figure 2. The hyper-viscoelastic model in Hexagon Marc is defined as illustrated in Figure 1.

The following assumptions were made to simplify the analysis of the FE model:

- The effects of drilling the holes through the aluminium end caps and putting the pins through were assumed to be negligible.
- The mass of nuts and bolts used to mount the vibration isolator onto the shaker and to attach to the 2 kg mass was assumed to be negligible.
- There was full contact between the aluminium and the silicone rubber, as well as between the isolator and the base, and between the top mass and the aluminium end caps.

Assumptions were based on existing research and validated through small changes in correlation with each increment. In the first assumption, the mass of material lost by drilling the hole was replaced by the mass of the aluminium pin going through the hole. The second assumption considered the mass of the nuts and bolts as a small fraction (3.6 %) of the total isolator mass. For the final assumption, contact was promoted by adding the aluminium pins and the interlocking design of the endcaps.

The FE model was set up such that all the degrees of freedom at the interface between the aluminium and the silicone rubber material were shared. First-order hexahedral elements were subsequently applied to the geometry. A mesh convergence study revealed that an element size of 4 mm was adequate. For hyperelastic elements and full integration, it is highly recommended to use the Herrmann formulation of the Type 84 hexahedral element in Hexagon Marc. FE model convergence was assessed by monitoring residuals and displacements, with tolerances set to 0.001. The 2.14 kg mass applied to the vibration isolator was represented as a point mass. This point mass was evenly distributed on the top surface of the vibration isolator without adding any stiffness using rigid elements (RBE3s). The central node was positioned at the centre of gravity of the applied mass, which is offset from the vibration isolator's surface.

A base acceleration load measured from the physical experiment was implemented as a time-history table in Hexagon Marc. This acceleration was applied to all the nodes at the bottom surface of the geometry. To address potential rigid body modes and avoid over-constraining the model, the centre node displacements in the $x-$ and $y-$ directions were constrained, and at the same $x-$ distance, the $y-$ displacement at the edge node was constrained. A timestep refinement analysis was done to ensure the correct timestep was used; a timestep of 40 timesteps per sine wave proved to be sufficient. The large-strain parameter was used to perform a nonlinear dynamic transient analysis over a total time of 5 s.

6 Results and discussion

The validation experiments in Section 5 were done at a sampling frequency of 256 Hz across all tests. Figure 10 presents the results from the test conducted at 5 Hz.

http://dx.doi.org/10.69694/2309-8988/2025/v41a4
http://www.saimeche.org.za (open access) © CC BY 4.0

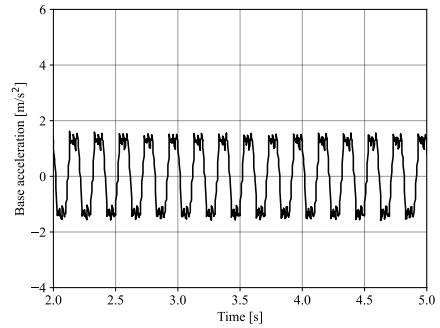

(a)

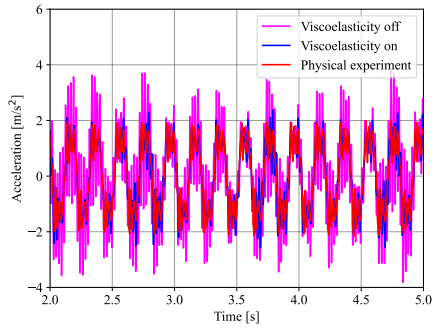

(b)

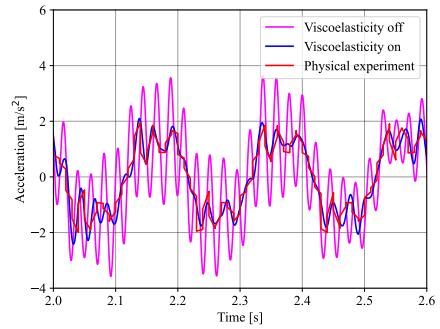

(c)

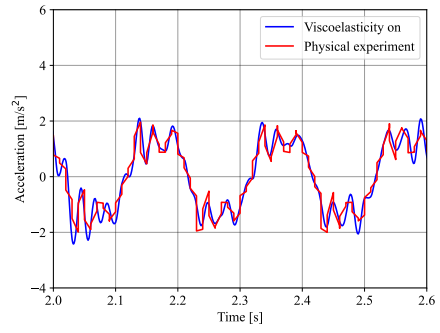

(d)

Figure 10 Material characterisation validation results at 5 Hz. Image (a) presents the system's base acceleration. Image (b) compares the experimental and simulated results, both with and without damping, while image (c) provides a detailed view of image (b). The significance of damping is emphasised in image (d), where the simulation with damping closely aligns with the experimental data

The simulation that excludes viscoelastic behaviour (no damping) deviates significantly from the experimental results. Simulations that include both hyperelastic and viscoelastic properties (with damping) show much closer agreement with the experimental data, highlighting the importance of damping for accurately modelling the system. Without the damping effect of viscoelasticity, the system appears to overestimate oscillations, whereas damping helps replicate the experimental system's actual behaviour.

Figure 11 compares the experimental and simulation results at varying frequencies with the viscoelastic behaviour accounted for. At frequencies of 10 Hz to 15 Hz, the correlation remained strong, suggesting that the simulation model captures the dynamics of the isolator well. However, at 25 Hz, the differences became more visible, indicating that the model may face limitations at higher frequencies. This divergence was expected, given that the viscoelastic parameters for the silicone rubber were derived from a quasi-static relaxation test [13].

http://dx.doi.org/10.69694/2309-8988/2025/v41a4
http://www.saimeche.org.za (open access) © CC BY 4.0

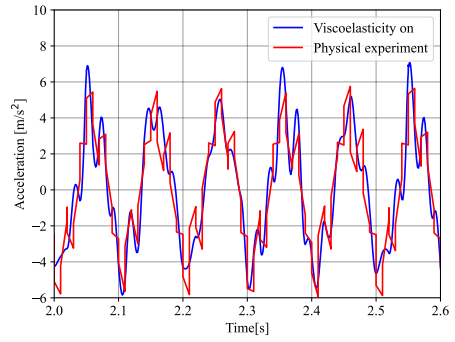

(a) 10 Hz

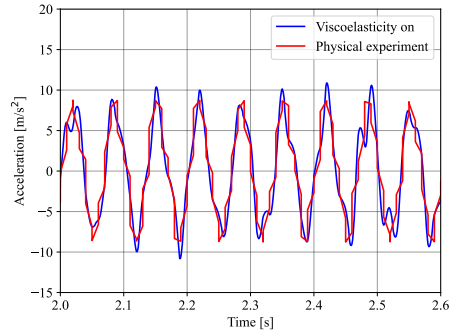

(b) 15 Hz

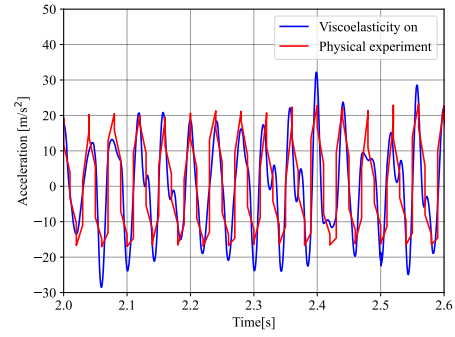

(c) 25 Hz

Figure 11 Comparison of acceleration results from physical experiments and Marc simulations at varying frequencies. Image (a) shows the acceleration response at 10 Hz, (b) response at 15 Hz and (c) response at 25 Hz

To validate the material characterisation results in the frequency domain, a fast Fourier transform (FFT) was applied to the time series data. The FFT transforms the time-domain signal into its frequency components, enabling a detailed comparison of the dominant frequencies and harmonics within the dataset [14]. Figure 12 illustrates the validation results at 10 Hz, 15 Hz and 25 Hz in the frequency domain, emphasising that the validation works at low frequencies and differences are more prominent at about 25 Hz.

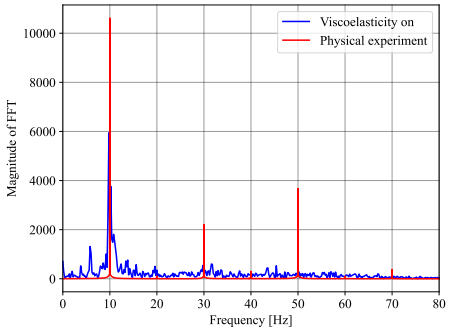

(a) 10 Hz

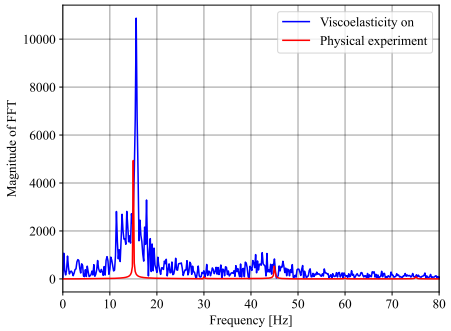

(b) 15 Hz

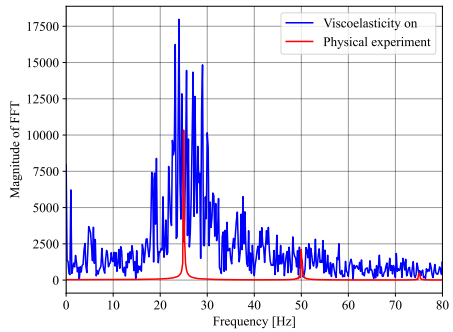

(c) 25 Hz

Figure 12 Frequency-domain comparison of experimental results and Marc simulations. (a) response at 10 Hz (b) response at 15 Hz and (c) response at 25 Hz

7 Conclusions

This project aimed to develop a methodology for characterising and modelling the hyperelastic and viscoelastic properties of rubber. The literature revealed that there are several ways to do this. For the hyperelastic characterisation, an indentation test with DIC data collection was conducted to obtain deformation data. A three-parameter Mooney-Rivlin model was selected and characterised by performing inverse FE mod-

http://dx.doi.org/10.69694/2309-8988/2025/v41a4
http://www.saimeche.org.za (open access) © CC BY 4.0

elling, tuning and updating the FE model to match the experiment to obtain the hyperelastic parameters of silicone rubber. The viscoelastic parameters were determined using a single quasi-static relaxation test, and a four-parameter Generalised Maxwell model was selected to fit the data. The hyperelastic material model was expanded in the FE software to incorporate the viscoelastic behaviour, creating a hyper-viscoelastic model.

To validate the material characterisation, a physical experiment was done, which used a different geometry and loading condition compared to how the material was characterised. It consisted of a base acceleration applied to a custom-designed and manufactured vibration isolator, which had a mass attached at the top. A FE model was made to replicate the physical test. Although literature indicated that the viscoelasticity of the unfilled silicone rubber would be low, the results revealed that the viscoelasticity in the system was crucial to accurately capture the dynamic behaviour of the material. It was also determined that the material characterisation was effective up to a point; at low frequencies such as 10 Hz the simulated data had good correlation with the experimental data. As the frequency of the applied load was increased, the difference between the simulated and experimental data became larger and at about 25 Hz this difference became significant.

References

[1] X. Liao, H. Xu, S. Li, C. Zhou, G. Li, and C.B. Park, *The effects of viscoelastic properties on the cellular morphology of silicone rubber foams generated by supercritical carbon dioxide*, RSC Adv., The Royal Society of Chemistry, vol. 5, no. 129, pp. 106981-106988, 2015.

[2] J. Bergstrom, *Preface*, in *Mechanics of Solid Polymers*, William Andrew Publishing, pp. xiii–xiv, 2015.

[3] W.N. Findley, J.S. Lai, and K. Onran, *CHAPTER 8 - Nonlinear Creep at Constant Stress and Relaxation at Constant Strain*, in *Creep and Relaxation of Nonlinear Viscoelastic Materials*, North-Holland, North-Holland Series in Applied Mathematics and Mechanics, vol. 18, pp. 176–219, 1976.

[4] Y. Li, S. Chen, J. Chen, S. Shi, and L. Peng, *A Hyper-viscoelastic model for filled-rubber materials: experiments and simulations*, Journal of Physics: Conference Series, IOP Publishing, vol. 1774, no. 1, p. 012066, 2021.

[5] R. Dhakad, D. R. Hipparkar, A. Kumar, and S. Chandel, *A hyper-viscoelastic constitutive model for elastomers: A case study of hydrogenated nitrile butadiene rubber and polychloroprene rubber*, Journal of Elastomers & Plastics, vol. 55, no. 7, pp. 1013–1034, 2023.

[6] J.D. Van Tonder, *Using Full Field Data to Produce a Single Indentation Test for Fully Characterising the Mooney-Rivlin Material Model*, PhD dissertation, 2023.

[7] T. Rey, G. Chagnon, J.-B. Le Cam, and D. Favier, *Influence of the temperature on the mechanical behaviour of filled and unfilled silicone rubbers*, Polymer Testing, vol. 32, no. 3, pp. 492-501, 2013.

[8] M. Hajhashemkhani, M.R. Hematiyan, and S. Goenezen, *Identification of hyper-viscoelastic material parameters of a soft member connected to another unidentified member by applying a dynamic load*, International Journal of Solids and Structures, vol. 165, pp. 50-62, 2019.

[9] M. Wadham-Gagnon, *Hyperelastic modelling of rubber behaviour in finite element software*, Master's Dissertation, McGill University, 2008.

[10] BSI Standards Limited, *Rubber, vulcanised or thermoplastic — Determination of ageing characteristics by measurement of stress relaxation in tension*, BS ISO 6914:2021, Published by BSI Standards Limited, 2021.

[11] BSI Standards Limited, *Rubber, vulcanised or thermoplastic — Determination of tensile stress-strain properties*, BS ISO 37:2017, Published by BSI Standards Limited, 2017.

[12] R. Budynas and K. Nisbett, *Shigley's Mechanical Engineering Design*, McGraw-Hill Higher Education - VST E+p, 2014.

[13] H. Ucar and I. Basdogan, *Dynamic characterisation and modeling of rubber shock absorbers: A comprehensive case study*, Journal of Low Frequency Noise Vibration and Active Control, vol. 37, no. 3, pp. 509-518, 2018.

[14] M. Cameron , *Fourier Transforms With scipy.fft: Python Signal Processing*, Real Python, 2020.

http://dx.doi.org/10.69694/2309-8988/2025/v41a4
http://www.saimeche.org.za (open access) © CC BY 4.0